Bioactive Materials 5 (2020) 447–457

Contents lists available at ScienceDirect

Bioactive Materials

journal homepage: http://www.keaipublishing.com/biomat

Metal alginates for polyphenol delivery systems: Studies on crosslinking ions and easy-to-use patches for release of protective flavonoids in skin

João Silva[a], Pavlo Vanat[a], Dorinda Marques-da-Silva[a], Joaquim Rui Rodrigues[a,b], Ricardo Lagoa[a,c,*]

[a] School of Technology and Management, Polytechnic Institute of Leiria, Portugal
[b] Laboratório Associado LSRE-LCM, School of Technology and Management, Polytechnic Institute of Leiria, Portugal
[c] UCIBIO-Faculty of Science and Technology, NOVA University of Lisbon, Portugal

ARTICLE INFO

Keywords:
Topical drug delivery
Intrinsic viscosity
Biopolymer
Epigallocatechin-gallate
Antioxidant dressing

ABSTRACT

Incorporation of bioactive natural compounds like polyphenols is an attractive approach for enhanced functionalities of biomaterials. In particular flavonoids have important pharmacological activities, and controlled release systems may be instrumental to realize the full potential of these phytochemicals.

Alginate presents interesting attributes for dermal and other biomaterial applications, and studies were carried here to support the development of polyphenol-loaded alginate systems. Studies of capillary viscosity indicated that ionic medium is an effective strategy to modulate the polyelectrolyte effect and viscosity properties of alginates. On gelation, considerable differences were observed between alginate gels produced with Ca^{2+}, Ba^{2+}, Cu^{2+}, Fe^{2+}, Fe^{3+} and Zn^{2+} as crosslinkers, especially concerning shrinkage and morphological regularity. Stability assays with different polyphenols in the presence of alginate-gelling cations pointed to the choice of calcium, barium and zinc as safer crosslinkers. Alginate-based films loaded with epicatechin were prepared and the kinetics of release of the flavonoid investigated. The results with calcium, barium and zinc alginate matrices indicated that the release dynamics is dependent on film thicknesses, but also on the crosslinking metal used.

On these grounds, an alginate-based system of convenient use was devised, so that flavonoids can be easily loaded at simple point-of-care conditions before dermal application. This epicatechin-loaded patch was tested on an *ex-vivo* skin model and demonstrated capacity to deliver therapeutically relevant concentrations on skin surface. Moreover, the flavonoid released was not modified and retained full antioxidant bioactivity. The alginate-based system proposed offers a multifunctional approach for flavonoid controllable delivery and protection of skin injured or under risk.

1. Introduction

The development of bioactive materials incorporating natural polyphenols is growing at a rapid pace. Applications were previously reviewed by Shavandi et al. (2018) and include skin patches, wound closure, coatings, coordination nanomaterials, theranostics and engineered tissue substitutes [1–6]. More recently, Yu and colleagues (2019) prepared titanium oxide composites with curcumin, quercetin and catechin, which showed radical scavenging capacities similar or superior to those of the composites with vitamin E [7]. Alginate matrices have been less employed, but catechin showed partial protective effects on chondrocytes seeded on alginate-chitosan scaffolds [8], and incorporation of icariin or chlorogenic acid into chondrocyte-alginate hydrogel systems enhanced articular cartilage repair in animal models [9,10]. Alginate-chitosan nanoparticles loaded with quercetin showed antioxidant activity in different *in vitro* models and a good safety profile *in vivo* [11].

Innumerous delivery systems have been developed aiming to improve the bioavailability and therapeutic efficiency of polyphenols and other phytochemicals. Some specific vehicles are designed exploring mucosal and dermal delivery to achieve high concentrations of the active compounds at target tissues such as brain, colon or skin, a strategy that is particularly interesting for polyphenol-based therapies [6].

Peer review under responsibility of KeAi Communications Co., Ltd.
* Corresponding author. School of Technology and Management, Polytechnic Institute of Leiria, Portugal.
E-mail address: ricardo.lagoa@ipleiria.pt (R. Lagoa).

https://doi.org/10.1016/j.bioactmat.2020.03.012
Received 22 November 2019; Received in revised form 22 March 2020; Accepted 23 March 2020

Polyphenols in general are recognized as antioxidant and anti-inflammatory agents, showing in varying degree anticancer, neuroprotective and other health promoting effects [6,11–13]. There is a great diversity of polyphenols, from phenolic acids like gallic acid, to curcuminoids and stilbenes (resveratrol). Gallic acid has anti-inflammatory and anti-toxic actions [14] and, *in vitro*, concentrations inferior to 100 μM (between 4.8 and 13.2 μg/mL) killed cancer cells without affecting hepatocytes [15]. Flavonoids are a major group of polyphenols, including lead compounds such as quercetin and the tea catechins (epi)catechin and epigallocatechin-3-gallate (EGCG). A recent cohort study revealed the association of quercetin and epicatechin consumption with a lower risk of mortality among participants with at least one risk factor [16]. It is important to note that pharmacological activities of flavonoids are expected typically at concentrations between 1 and 50 μM [4,6,11].

Incorporation of gallic acid, resveratrol, curcumin, genistein, quercetin and tea catechins into (bio)polymer films, particles and other carriers attracts significant attention in the development of bioavailability-enhancing and therapeutic anticancer delivery systems [6,11]. Green tea and derived polyphenol-rich extracts showed promising anticancer results in some clinical trials and EGCG is a top potential chemopreventive agent with high level of evidence for melanoma prevention [6,17]. Moreover, a catechin preparation consisting of an ointment with a standardized extract of green tea leaves from *Camellia sinensis* containing tea polyphenols (sinecatechins) is already approved for topical use in humans for treating warts (Veregen™, PharmaDerm). The treatment consists of three daily applications of the ointment up to 16 weeks. Meanwhile, a phase 2 trial of Veregen for the treatment of basal cell carcinoma (total of 42 patients, application twice daily) noticed some antitumor action, but not statistically significant [18]. Surprisingly, this trial reported erythema and edema adverse effects, whereas topical application of catechins was previously indicated to decrease erythema conditions [17], all suggesting that dosing regimen may be critical for the treatment outcome and optimized dermal delivery systems are necessary. In this line, a previous simulation study of catechins' dermal penetration recommended skin surface concentrations of approximately 25 μM for high anticancer activity and, simultaneously, avoiding potential toxic effects at the dermis layer [19].

In addition to anticancer potential, other clinical trials, epidemiological and laboratory studies give strong support to the beneficial effects of epicatechin and tea catechins in skin protection [20–22], cardiovascular health [23–25] and against neurodegenerative diseases [13]. Oral administration in humans showed that catechins can reach the skin, but at lower levels than in plasma and with significant metabolization and interindividual variation [21,22]. Although human trials generally find no side effects of interventions with green tea [21,26], concerns regarding the hepatotoxicity of concentrated extracts that boost oral bioavailability were published very recently [27]. In alternative, dermal delivery is an attractive option to control pharmacologically relevant and non-toxic concentrations of tea catechins and other protective flavonoids in skin.

The polysaccharide alginate is appraised for producing biomedical materials due to its good biocompatibility, relative low cost and amenable gelation with divalent cations [28–30]. Concerning dermal applications, the biopolymer's ability to maintain a moist environment or absorb excess fluid is useful for wound healing [31]. Therefore, alginate is an interesting carrier for novel polyphenol delivery systems, but the possible use of different gelling cations and other factors affecting the delivery abilities of alginate matrices should be considered. Jiang and colleagues (2013) used the internal gelation technique to load rutin in chitosan-coated alginate microcarriers and, although a sustained release system was produced, several steps were demanded [32]. Shrinkage during gelation (syneresis) can be a drawback of alginate and efforts are devoted to control it on the fabrication of tridimensional (3D) structures [33,34]. Using copper ions as crosslinker, we observed before that higher polysaccharide/cation ratios generate gels with a greater water content and less rigid [35], and a similar result was observed with zinc-induced gels [36].

Alginate is also less employed in 3D printed drug delivery systems [37,38], probably because of the printability difficulties of alginate usually crosslinked with calcium ions. A suitable viscosity is a top requisite for printing technologies and varying the gelatin ratio in mixtures with alginate was explored to optimize printing parameters [39]. Polyethylene oxide and Triton X-100 were also used to modulate the viscosity properties of alginates and improve their spinnability [40]. However, apparently divergent results of alginate viscosity properties have been observed in different studies. While non-linear changes of reduced viscosity with polymer concentrations have been discussed by some authors [41–43], other studies report no such deviations [40,44,45]. Moreover, in addition to the so-called "polyelectrolyte effect" [43], adsorption of the alginate polymer onto capillary walls was also described to cause an increase of reduced viscosity with decreasing polymer concentration [42] and might affect fluid dynamics in printing spinnerets [33]. Recently, Dodero et al. (2019) underlined that the viscosity properties, namely concentration regimes and polyelectrolyte nature, will be influenced by the monomer composition and molecular mass of alginates [40]. Nevertheless, the influence of biopolymer concentration and medium ionic strength in viscosity deserves further investigation to overcome difficulties in the production of complex alginate structures, and this prompted us to carry out capillary viscosity studies in this work.

Alginate hydrogels are most commonly produced by ionic crosslinking using calcium cations, including for 3D and polyphenol-loaded structures [9,10,33,46]. However, other metal cations (Cu^{2+}, Zn^{2+}, Sr^{2+}, …) are increasingly explored in novel production techniques or to tailor the properties of alginates in the development of new functional biomaterials, namely for antibacterial and bone tissue regeneration [36,46–51]. In addition, published data indicate that by selecting the gelling cation (zinc *vs* calcium) it is possible to tune the drug release properties of alginate systems [52,53].

The aims of the present work were to investigate the suitability of different metal ions in the production of alginate structures for polyphenol encapsulation and the development of an easy-to-use dermal delivery system suitable for future flavonoid treatments.

2. Methods

2.1. Alginates and chemicals

Sodium alginates from two different suppliers were tested in this work: one purchased from Panreac (catalog number 373059.1209) and another from Sigma (catalog number A2033, medium viscosity, from *Macrocystis pyrifera*), and hereinafter referred to as alginate P and alginate S, respectively. Average molecular weight was calculated from the intrinsic viscosity using the Mark–Houwink parameters $K = 7.3 \times 10^{-5}$ and $a = 0.92$ [40,44]. The values obtained, 351×10^3 g/mol for alginate P and 428×10^3 g/mol for alginate S, are within the order of magnitude of algae-sourced alginates used in biomedical applications [40,41,45,54,55].

Metal chlorides were obtained from Merck. Polyphenols gallic acid (G7384, > 97%), epicatechin (E1753, > 90%) and EGCG (93894, ≥98%), cytochrome *c* (C7752) and all other chemicals and solvents were supplied by Sigma-Aldrich (St. Louis, Missouri, USA).

Solutions of alginates with concentrations 0.2, 1 or 2% (m/v), equivalent to g/dL, were prepared by dissolving a weighted amount of sodium alginate in a volume of deionized water, followed by agitation overnight. During the course of this work, at least 6 separate solutions of each alginate were prepared and used for viscosity measurements, gelation assays and preparation of films. Experimental solutions with lower concentrations were prepared by dilution of the stock solutions in deionized water.

2.2. Viscosity measurements

The apparent viscosities of alginate solutions were measured with a rotational viscometer Viscotech Myr model V1, using spindle L1 and two different speeds, at 20 °C. The intrinsic viscosities were obtained with a capillary viscometer having 0.5 mm capillary diameter and a solvent flow time (100 mM NaCl) of 127.3 s at 40 °C. Solutions of alginate P and S in deionized water and in 100 mM NaCl were used. For measurement, the solution was loaded into the viscometer immersed in a 40 °C circulating water bath, and the flow time was used to calculate the absolute viscosity (μ, mPa·s or cP):

$$\mu = Cv * t * d \quad (1)$$

where Cv is the viscometer constant (0.0072304 cSt/s), t is the flow time (s) and d is the solution density (g/cm^3). Equal measurements were carried with the alginate solutions and the corresponding solvents (deionized water and 100 mM NaCl). Flow time values were superior to 60 s in all measurements.

The specific viscosity (η_{sp}) was computed from the absolute viscosities of the polymer solution and the corresponding solvent:

$$\eta_{sp} = \frac{\mu\ solution - \mu\ solvent}{\mu\ solvent} \quad (2)$$

The reduced viscosity (η_{sp}/c, dL/g) is the quotient of the specific viscosity of the solution by the polymer concentration (c, g/dL), and the intrinsic viscosity, [η], is defined by the Huggins equation [43,45,56]:

$$[\eta] = \lim_{c \to 0} \frac{\eta_{sp}}{c} \quad (3)$$

2.3. Gelation studies using different metal ions

Alginate gels were prepared with diverse crosslinking metal ions, Ca^{2+}, Ba^{2+}, Cu^{2+}, Fe^{2+}, Fe^{3+} and Zn^{2+}, all as chloride salt solutions of 100 mM concentration. For gelation, 10 g of solution of sodium alginates S or P at 1% and 2% concentrations (w/v) in water, were placed in round molds of 9 cm diameter. Then, 20 mL of the metal solutions were gently added and the molds were maintained levelled and resting through 24 h. After this time, the remaining solution was collected, the gel superficial liquid in excess was absorbed with paper, and the gel structures immediately photographed and weighted.

The upper surface area of the gel discs produced was calculated from the digital photograph, using the image analysis software *ImageJ* [57]. The pH of the metal gelling solutions was measured with a HANNA HI3221 potentiometer. The acid Ca^{2+} solutions for alginate gelation were obtained by addition of small volumes of hydrochloric acid until a pH similar to the copper and iron ions solutions was reached (pH approximately 2–3, Table S.1).

For determination of the water content of gels, after weighting (m_{gel}), these were dried in an oven at 50 °C for a minimum of 5 days and until constant weight (less than 10% change from previous day mass). The last mass weighted (m_{dry}) was used to calculate the water content [%, (m_{gel}-m_{dry})x100/m_{gel}].

To study the stability of metal-alginate gels, dried and weighted gels were immersed in 20 mL deionized water or in saline medium (NaCl 150 mM, 0.9%). After 7 days, alginates were recovered, visually examined and dried until constant weight.

2.4. Quantification and stability of polyphenols in the presence of alginate-crosslinking metals

Stock solutions of the polyphenols were routinely prepared in dimethyl sulfoxide (DMSO) and diluted to the target concentrations just before use. Different methods were used to analyze the polyphenols: UV–Vis spectrophotometry, polyphenol assay and HPLC. Epicatechin was analyzed using UV–Vis spectrophotometry, by reading molecular absorption at 278 nm in a Varian Cary 50 spectrophotometer using 10 mm path length cuvettes. Standard curves were routinely constructed from epicatechin solutions with known concentrations up to 100 μM in water or saline and showed good linearity (correlation coefficients greater than 0.998). Concentration of unknown samples was obtained by interpolation of the corresponding absorbance at 278 nm on the standard curves. The total polyphenol assay was adopted from Ganesan et al. (2008). Briefly, 100 μL of sample was added to 2 mL of Na_2CO_3 (2% m/v), homogenized and, after resting for 2 min, 100 μL of Folin-Ciocalteu reagent (50% v/v) was added, homogenized and the absorbance at 720 nm measured once incubated for 30 min at room temperature in the dark [58]. EGCG and epicatechin were also quantified by phase reverse HPLC in an Agilent 1100 system equipped with a C18 column, and using a mobile phase consisting of triethylammonium phosphate:water:acetonitrile 1:83:16 (pH 4.3), flux 0.6 mL/min, and UV detection at 278 nm.

The stability of gallic acid, epicatechin and EGCG in presence of metal ions was studied with 100 μM solutions in saline medium (NaCl 150 mM). Absorption spectra of polyphenol solutions were collected in the range 200–600 nm, with a 1 nm resolution, then small volumes of metal solutions were added to the cuvette, homogenized and spectra was recollected (mixture polyphenol + metal ions). Assays were carried with 100 μM metal ions (1 min reaction time) and 500 μM metal ions (5 min reaction time) to examine possible changes in the absorption spectra of polyphenols. Difference spectra of the polyphenols in the presence of the metals were obtained by subtracting the absorption spectra of the metal solutions (at the corresponding concentration) from the spectra of the mixture (polyphenol + metal ion).

In another set of stability tests, EGCG at a concentration of 10 mM was mixed with metal ions (200 mM) and incubated for 20 h, at 4 or 20 °C. Initial and final mixtures were analyzed by HPLC. Chloride salts of the metal cations were used in all the stability studies as in the gelation of alginates.

2.5. Epicatechin loading into metal alginate matrices and release studies

The kinetics of release of epicatechin by alginate gelled using different crosslinking metal ions was studied with films of alginate having identical surface area (143 mm^2 in total, dry film).

Dry alginate films were prepared by casting so that films with two different thicknesses were obtained. Sodium alginate S (2% w/v) solution was distributed on a mold in two volume/area ratios (0.79 and 1.59 mL/cm^2 of base). After drying for 6 days at 40 °C, alginate films with 85 ± 12 and 202 ± 55 μm thicknesses and, respectively, with 1.5 ± 0.2 and 1.2 ± 0.4 mg/mm^3 apparent density were obtained and identified as thin and thick films. In the studies reported in this work, for each membrane thickness, a total of 3 batches of membranes were produced using separate solutions of alginate.

Epicatechin was encapsulated by addition to the crosslinking metal solutions used to gel the alginate films. For gelation, the dry sodium alginate films were immersed in a small volume of calcium, zinc or barium chloride 200 mM, for 18 h at 4 °C. Blank films were gelled in the absence of epicatechin, while epicatechin-loaded films were gelled with crosslinking metal solutions containing 0.57 μmol of the flavonoid. After gelation and encapsulation, the films were washed (three times for 1 s) in 1 mL of saline, and placed in 5 mL of saline solution (NaCl 150 mM) for monitoring epicatechin release under gentle agitation. Blank alginate matrices gelled with each metal were also assayed in parallel for Control. Samples of the release medium were withdrawn at time intervals and epicatechin quantified by molecular absorption (278 nm). In addition, the concentration in the saline at the end of the assays was confirmed (maximum difference 10%) by the polyphenol assay or by HPLC, as described in the previous section.

The kinetics of epicatechin release was studied by fitting the experimental data to the first order, Korsmeyer-Peppas and Weibull models [59]:

First order model: $C/C_\infty = 1 - e^{-kt}$ (4)

Korsmeyer − Peppas model: $C/C_\infty = kt^n$ (5)

Weibull model: $C/C_\infty = 1 - e^{-at^b}$ (6)

where k is the rate constant, n is an exponent related to the release mechanism, and a and b are constants. The mathematical models were compared by the adjusted coefficient of determination (R^2_{adj}) calculated with MATLAB as:

$$R^2_{adj} = 1 - \frac{(e-1)}{(e-p)}(1-R^2) \quad (7)$$

where e is the number of experimental points in the kinetic curve, p is the number of parameters in the model equation and R^2 is the coefficient of determination.

Skin delivery was studied in an *ex vivo* model using pig skin collected in a local abattoir and used less than 6 h after animal sacrifice. Calcium alginate thin films with encapsulated epicatechin were prepared as above. The skin was placed in a horizontal base, a small superficial incision (1 mm deep) was made, 100 μL of saline were dropped over the incision and, then, an epicatechin-loaded film was applied covering completely the incision. Control assays without any film and with Blank (no-flavonoid) films were run in parallel. After 1 h, the films were gently removed, the incision and skin covered by the film was sampled with 100 μL of saline rapidly collected to a microtube and frozen or maintained refrigerated for less than 3 h until analysis. The samples were centrifuged at 10 000 g for 5 min, and the supernatant analyzed for the epicatechin concentration by HPLC and antioxidant bioactivity.

Antioxidant bioactivity was measured by the cytochrome *c* reduction assay [12]. The samples were added to 10 mM phosphate buffer pH 8.0 supplemented with cytochrome *c* (20 μM final concentration), and the kinetics of reduction of the protein was followed by absorbance readings at 550 nm. In the case of the samples from skin exposed to blank films, after confirming the absence of antioxidant bioactivity, they were spiked with epicatechin at concentrations similar to those measured in samples from loaded films and cytochrome *c* reducing activity measured for comparison.

3. Results and discussion

3.1. Viscosity studies

This work employed two commercial alginates that have been used by different authors in the development of alginate-based biomaterials [35,40,54,60], alginates S and P specified in Methods section 2.1.

The viscosity of alginate solutions is a critical parameter in the production of alginate-based materials and some seeming divergent results have been reported in the bibliography, namely regarding the relevance of the "polyelectrolyte effect" or the adsorption of polymer chains on capillary surfaces [42,43].

Initially, we measured apparent viscosities of the two alginates, as described in Materials and Methods section. The results represented in Fig. 1 of Supplementary Data (Figure S.1) show that viscosity of alginates increased approximately linearly with concentration from 0.02 to 0.1 g/dL (or % m/v). Because the alginates exhibited very similar apparent viscosities, we proceeded to capillary viscosity studies and determination of their intrinsic viscosities.

Intrinsic viscosity is a measure of the hydrodynamic volume of the polymers at infinite dilution in a certain solvent. To investigate the influence of ions present in the solvent, alginate solutions in deionized water and 100 mM NaCl were compared. Absolute viscosities were measured and, then, specific and reduced viscosities were calculated as explained in the Materials and Methods section. Results indicate that alginate S is quite more viscous than alginate P, with absolute viscosities of 5.4 ± 0.1 and 4.6 ± 0.1 mPa s at 0.1 g/dL in water, respectively. Fig. 1 shows that absolute viscosities increase with alginate concentration both in the absence (panel A) and in the presence of NaCl (panel B). These plots suggest that the concentration dependence is not linear, and the deviations become more evident when plotting the specific viscosity (not shown) or the reduced viscosity (Fig. 1C and D). The deviations from linearity can be a consequence, at least in part, of the chain entanglement at low/intermediate concentrations [40].

All the data indicates that salt in the medium decreases markedly the biopolymer viscosity, probably because interactions of alginate chains with mobile ions Na^+ and Cl^- alter the molecular arrangement of the polysaccharide [56]. Interestingly, in the presence of salt, we could observe the constant increase of reduced viscosity at higher concentrations, as expected, but for more diluted solutions the reduced viscosity jumps to much higher values (Fig. 1D). The upward bending of reduced viscosity with dilution was also observed while studying the alginate solutions in deionized water and, in this case, it extended up to concentration 0.2 g/dL (Fig. 1C).

The linear increase in the reduced viscosity of NaCl alginate solutions for concentrations superior to 0.03 g/dL (trend lines in Fig. 1D) is the standard polymer behavior [44,45] and returned us the intrinsic viscosities of 11.1 ± 0.4 dL/g for alginate S and 9.2 ± 0.4 dL/g for alginate P by extrapolation of the reduced viscosity line to zero polymer concentration. These values are typical of medium/high viscosity alginates employed in biomaterial development [40,45,54]. Other authors reported this linear behavior of alginate solutions of intermediate/high concentrations, at least with NaCl solutions and alginate concentrations superior to 0.02 g/dL [44,45,56]. However, in different studies it was observed a curvature of reduced viscosity with alginate dilution that could span concentrations as 0.1 g/dL [41–43]. This observation is common with polyelectrolytes and interpreted as a "polyelectrolyte effect": alginate is a strong anionic polyelectrolyte and the electrostatic repulsion of charges in the same backbone (intra-chain) leads to chain extension and an increase of reduced viscosity with dilution [43,56]. Nevertheless, Zhong et al. (2010) presented an alternative explanation for that observation based on the adsorption of the polymer on glass capillary walls [42].

In our results, the presence of NaCl shows a potential useful influence on the increase of reduced viscosity upon dilution (Fig. 1C and D). The "polyelectrolyte effect" was much limited in the presence of salt (polymer concentrations < 0.02 g/dL), probably because it diminishes the alginate chains' charge density, hence weakening the repulsive electrostatic interactions and diminishing the propensity to assume rod-like conformation and behave as semi-rigid sticks [40]. In other words, small ions in alginate solution seem to favor a random coil conformation typical of neutral polymers. Without ruling out alternative explanations to the nonstandard increase in reduced viscosity at low alginate concentrations [42], our data and a previous study with alginate from *Lessonia nigrescens* [56] suggest that the "polyelectrolyte effect" is the dominant factor affecting such abnormality.

Yang and colleagues (2009) reported a similar action of a cationic surfactant in alginate solutions. The surfactant counteracted the polyelectrolyte behavior of alginate, dose-dependently attenuating the reduced viscosity increase at low alginate concentrations [41]. These authors argued that, at neutral pH, the cationic surfactant decreases the overall charge of carboxylic groups, the size of the anionic alginate chains and the intra-molecule repulsion, while enhancing intermolecular possible entanglements, hydrogen bonds and formation of association structures.

Although further studies would be needed to detail the effects on the molecular arrangement of the biopolymer chains, the present results point to the use of NaCl in alginate solutions as a practical means to modulate the viscosity properties. Physiological salt concentrations (0.9% m/v) are suitable for biological systems, may favor hydrogel stability [61] and provide an alternative to other additives [39–41] for

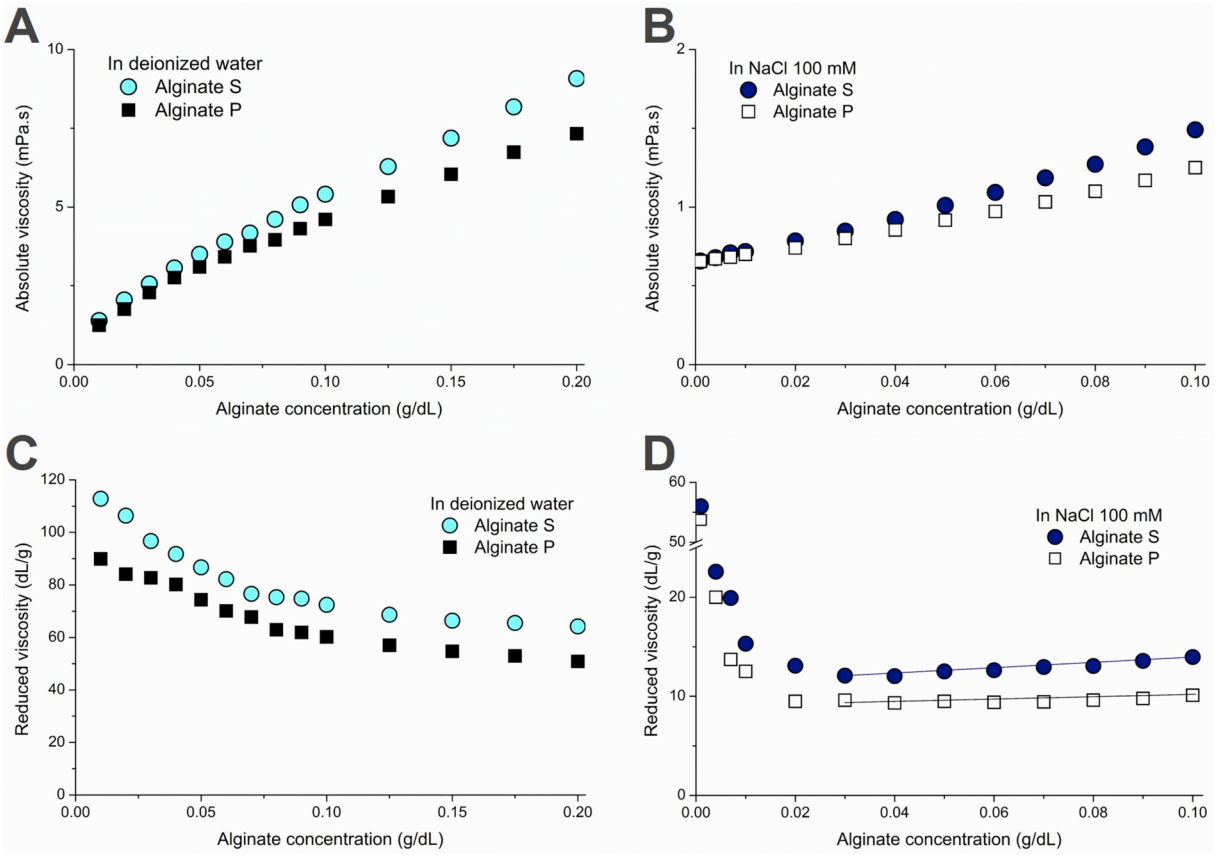

Fig. 1. Absolute viscosity (A and B) and reduced viscosity (C and D) of alginates S and P in deionized water and in 100 mM NaCl. Absolute viscosity increases with alginate concentration, both in absence and in presence of NaCl. Reduced viscosity decreases with biopolymer concentration, but in NaCl this decrease is limited to concentrations inferior to 0.02 g/dL. Measurements were carried out with two solutions of each alginate and the maximum standard error (SE) observed for reduced viscosity was 2.0 dL/g (relative SE 16%, with an alginate concentration 0.01 g/dL in NaCl). The straight lines in panel D correspond to linear regression fits of the experimental data and where used to obtain the intrinsic viscosities of the alginates (equation (3) in Methods).

easing the fabrication of complex alginate structures. The studies of alginate hydrogel formation and polyphenol encapsulation in simple geometries presented in the following sections were performed in the absence of NaCl, as chloride salt solutions of the crosslinking metal ions at 100 mM concentration were used and no further control of viscosity was needed.

3.2. Alginate gelation using different metal ions

One of the most interesting properties of alginate is the ability to obtain gel structures by reticulation with different metal ions in mild conditions. Discs of metal-alginates were produced using Ca^{2+}, Ba^{2+}, Cu^{2+}, Fe^{2+}, Fe^{3+} and Zn^{2+} added to sodium alginates S and P in concentrations 1% and 2% (w/v) in identical molds, and Fig. 2 shows photographs of typical gels obtained. The gels obtained with 1% alginates were generally very similar to the 2% (w/v), but some results of 1% gels are given in Supplementary Data for further discussion (Figure S.2).

Calcium, barium and zinc generated the more regular gels, at least with alginate S, while copper alginates tended to gel in uneven way and thus lose the round shape of the mold (Fig. 2). All the gels had enough resistance for common handling as removing from the mold and weighting, with exception of those obtained with Fe^{3+} and Fe^{2+} that could not be removed from the mold without breaking the fragile gel in parts. The gels formed with Fe^{2+} (not shown) and Fe^{3+} were similar, and remarkably gelled with low shrinkage (Figs. 2 and 3). To evaluate syneresis, the surface area and mass of the gels were measured and plotted in Fig. 3, showing that on typical gelation with Ca^{2+}, Ba^{2+} and Zn^{2+}, the initial 10 g sodium alginate solutions resulted in approximately 5 g gel discs with areas less than half that of the mold. The copper alginates were slightly bigger than those obtained with Ba^{2+} or Zn^{2+}, and their mass actually reached values similar to the iron-induced gels when sodium alginate in concentration 1% (w/v) was used (Figure S.2A).

In addition to viscosity of alginate flow, shrinkage in the gelling process is a major complication for printing, microfluidics and geometric control of alginate structures [33,34]. The differential shrinkage we observed in copper and iron-induced gelation suggests these crosslinking ions may be useful for production of alginates with improved geometric control. However, it should be remembered that alginate can also gel as alginic acid in acidic conditions [62], hence the gelation induced by copper and iron solutions might be influenced by the pH of these solutions.

Indeed, the copper and iron ions solutions used in alginate gelation were acidic, with pH values below 4 (Table S.1). To investigate this potential interfering factor, calcium solutions were acidified to pHs similar to the iron and copper solutions and used to gel alginate in the same conditions. After the 24 h gelation, the remaining calcium solutions preserved a pH acid and considerably lower than the non-acidified solution (Table S.1), but the calcium alginate gels formed in these dissimilar pH conditions don't show any significant differences (Figs. 2 and 3). These results suggest that the differences observed in the formation of iron and copper alginates are not due to the solution acidity, but more directly related to the metal ions interacting differently with alginate chains.

A closer look at the pH changes in the gelation baths (Table S.1) show that at the end of the process the pH of the remaining solutions was in general superior to the initial. All these changes were in the

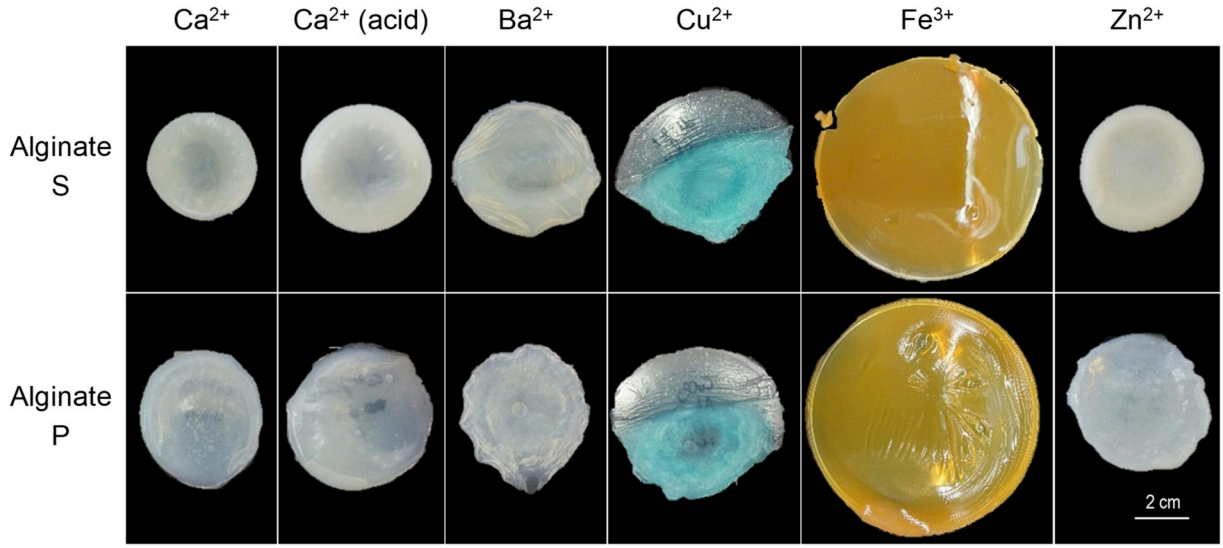

Fig. 2. Gels of alginates S and P obtained with different crosslinking metal ions. Sodium alginates (10 g, 2% w/v) in round molds (9 cm diameter) were gelled with 100 mM solutions of each metal. Photographs are representative of three gelation assays with each alginate and metal ion. Calcium-induced gelation was also studied using solutions acidified with HCl to pH = 2.3 ± 0.5.

direction of neutrality, as expected taking into account that the sodium alginate solutions had neutral pHs (7.0 ± 0.1 for alginate S and 6.5 ± 0.3 for alginate P). The only exception was observed in gelation of Zn-alginates that caused a small acidification of the medium.

There were no evident differences between the alginates S and P regarding the water content of the gels produced that was very high: most of the gels had 94–96% water, both starting with alginate solutions 2% (Fig. 3C) or 1% (w/v) (Figure S.2B). Although not reaching significant differences, some copper and iron-induced gels showed slightly higher water contents in accordance to the decreased syneresis (water and mass loss) on gelation.

The metal-alginate materials were further challenged by testing their stability in deionized water and in saline medium (NaCl 150 mM, 0.9%) simulating body fluids. This and the following studies were carried out only with alginate S, since it was the alginate giving more regular structures on gelation (Fig. 2). Gelation with Fe^{2+} was also not further studied since the formed gels were too brittle. After immersion in deionized water for 7 days, no visible changes were observed in any of the gels, but in saline medium the barium and zinc alginates became softer and more fragile. At least for zinc alginates, the stability can be improved through a post-gelation immersion in $CaCl_2$ [36]. We have also noticed the decrease in pH of both media (deionized water and saline) in the case of Fe^{3+} alginate, possibly because of leakage of the metal ions to the bathing solutions. Importantly, all alginates lost considerable mass throughout the assay, except calcium alginate that revealed a good stability in saline medium (Fig. 4).

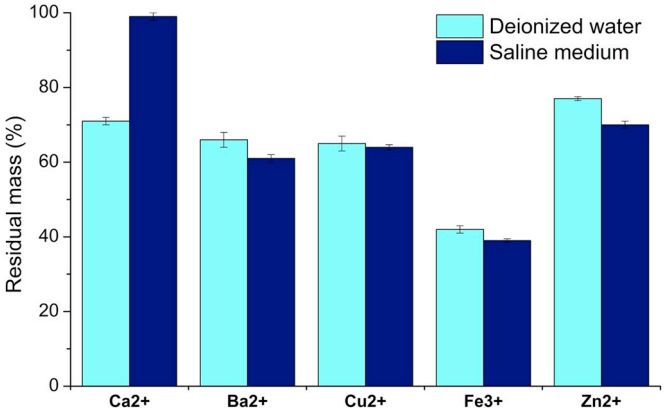

Fig. 4. Relative mass retention of metal alginates in deionized water and saline medium (NaCl 150 mM). All the metal alginates lost mass in the media tested, except for calcium alginate in saline. Data presented are the mean ± SE from triplicate gelation assays.

3.3. Stability of polyphenols in presence of alginate-crosslinking metals

Construction of polyphenol-loaded alginate gels requires the selection of reticulating metal ions compatible with polyphenols. Some metal ions and polyphenols are far from being chemically inert species, so this point can be critical for the design of delivery systems. We chose three polyphenols to investigate possible incompatibilities with metal cations: gallic acid as a prototypical simple polyphenol with a

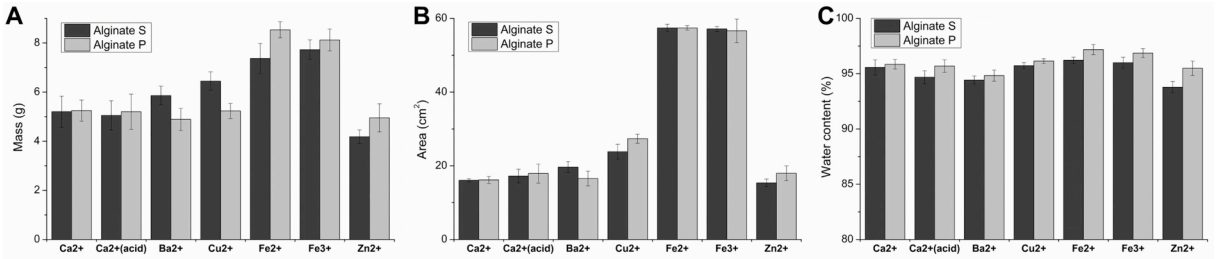

Fig. 3. Mass (A), upper surface area (B) and water content (C) of gels of alginates S and P obtained with different crosslinking metal ions. Details as in Fig. 2 caption and Methods. Calcium, barium and zinc induced extensive syneresis, as indicated by lower gel mass and surface area. Gelation with both iron ions Fe^{2+} and Fe^{3+} originated larger, but brittle, gels. All gels had similar water content and superior to 94%. Data presented are the mean ± SE from triplicate gelation assays.

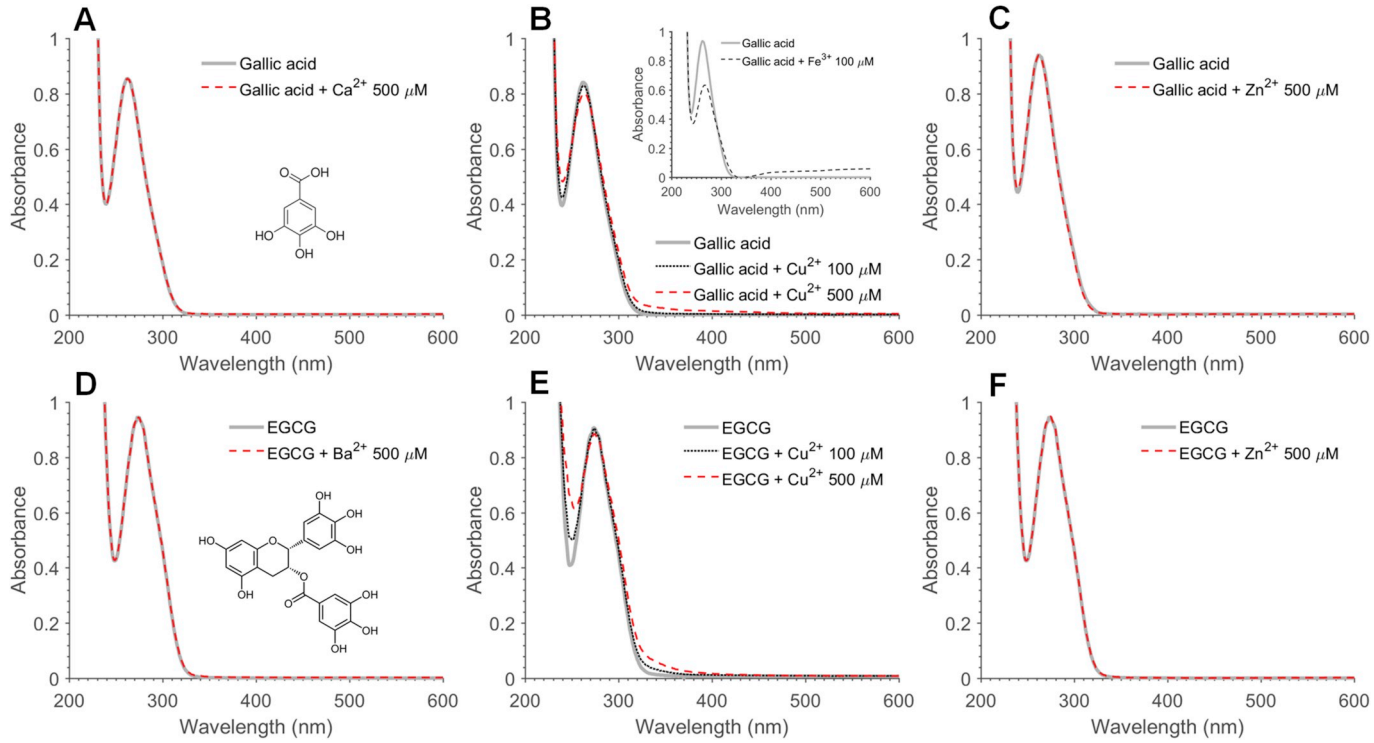

Fig. 5. Absorption spectra of 100 μM solutions of gallic acid (upper panels) and epigallocatechin-gallate (EGCG) (lower panels) in the absence (solid line) and in the presence (dotted or dashed line) of metal cations. The molecular structures of gallic acid and EGCG are shown in panels A and D, respectively. Further details in Methods. Spectra are representative of at least two assays with each polyphenol and metal ion. While calcium, barium and zinc do not alter the absorption spectra of the tested polyphenols, iron and copper do so, which suggests oxidation of the polyphenols by these metal ions.

pyrogallol ring, and epicatechin and EGCG as two chief bioactive flavonoids.

Having in mind the redox behavior of polyphenols, it is expectable that they are able to reduce certain oxidizing metal cations. In addition, flavonoids can form complexes with metal cations [4,63], so we probed the interaction between the polyphenols and alginate-gelling ions by UV–Vis spectrophotometry. Fig. 5 shows the absorption spectrum of gallic acid and EGCG with the UV absorption band typical of phenolic compounds and in the presence of metals used in alginate gelation. Representative spectra obtained with epicatechin are presented in Supplementary Data (Figure S.3). Calcium, barium and zinc ions caused no detectable alterations in the absorption spectra of the compounds, even when excess (1:5 ratio) concentration was used, as shown in Fig. 5 and S.3. On the other hand, both Cu^{2+} and Fe^{3+} induced changes in the spectra of the three polyphenols suggestive of oxidation, noticeable with 100 μM concentration of the metal ions (Fig. 5B and E, S.3B and S.3C).

The integrity of EGCG was also examined by HPLC that confirmed the transformation of the flavonoid in the presence of Cu^{2+} ions (Fig. 6). Analysis of the mixture of EGCG with Cu^{2+} showed that the chromatographic peak characteristic of EGCG decreased substantially compared with the control solutions without metal ions, and new peaks appeared in the chromatogram at shorter retention times plausibly due to degradation products of the flavonoid (Fig. 6A). The cupric and ferric ions-induced alterations in the absorption spectra of polyphenols, appearance of absorbance bands in the visible region (Fig. 5B and E), and changes in the chromatographic profile (Fig. 6A), even at low concentrations and in a short reaction time, indicate that these metal ions are incompatible with polyphenol loading into alginate materials due to redox reaction.

Considering the better compatibility of Ca^{2+}, Ba^{2+} and Zn^{2+} ions with polyphenols, we extended the stability studies to more challenging conditions identical to those used in alginate gelation, i.e. with higher concentrations and longer incubation times. This set of assays was

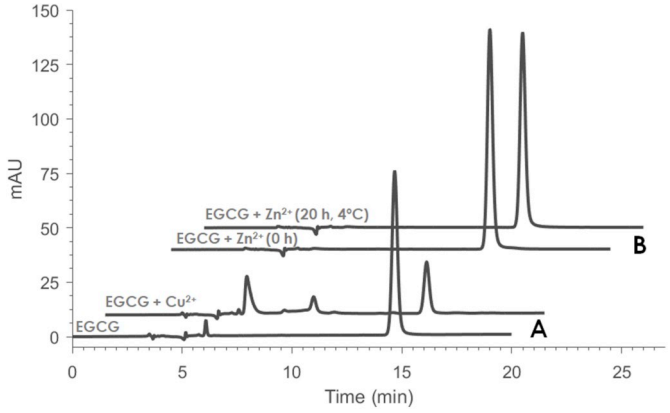

Fig. 6. Representative HPLC chromatograms for epigallocatechin-gallate (EGCG) analysis. The below pair of chromatograms (A) are EGCG (100 μM) in the absence and in the presence of equimolar copper (II) ions shortly after addition (at 20 °C). The above pair (B) are EGCG with zinc ions just after mixing (no incubation time, 0 h) and 20 h after incubation at 4 °C. For these latter chromatograms, the mixtures of EGCG (10 mM) and zinc (200 mM) were diluted 100 times before analysis. The chromatograms are presented displaced in the vertical and horizontal axes for better observation. Chromatograms shown are representative results of triplicate assays with each metal ion.

carried out with EGCG, which has a low redox potential, so it is more prone to oxidation [12]. The flavonoid was incubated with calcium and zinc ions (200 mM) for 20 h, exceeding the gelation time we used in the production of flavonoid-carrying films (section 2.5). After incubation at 4 or 20 °C, EGCG solutions with or without ion metals were analyzed by HPLC (Fig. 6B and Table 1). In any of the cases we noticed significant changes in the chromatographic profile of the flavonoid, as illustrated in Fig. 6B for the zinc mixture. Quantification of the flavonoid peak area from solution after incubation and comparison with the initial

Table 1
Stability of epigallocatechin-gallate in water and metal solutions in conditions identical to the gelation of alginate matrices (metal concentration 200 mM). Data presented are the mean ± SE from triplicate assays.

Temperature (°C)	Medium	Concentration decrease after 20h (%)
4	Deionized water	0.2 ± 1.3
	Ca^{2+}	1.9 ± 3.8
	Zn^{2+}	12.5 ± 1.0
20	Deionized water	0.0 ± 1.1
	Ca^{2+}	8.1 ± 4.9
	Zn^{2+}	3.8 ± 3.1

solution in deionized water demonstrated a good stability in water and in calcium mixture at 4 °C (Table 1). At 20 °C and in the zinc solution we detected slight decreases of EGCG concentration, eventually resulting from slow oxidation by trace iron ions from zinc chloride reagent and favored by zinc-flavonoid chelates [64].

To sum up, the results in this section clearly indicate that Cu^{2+} and Fe^{3+} ions should be avoided in biomaterials intended for polyphenol encapsulation. Fe^{3+} reacts readily with phenolic compounds and Cu^{2+} at the high (milimolar) concentrations used for alginate gelation should also be discarded. Copper-containing alginates have been tested for antibacterial materials [48,49], and eventually Cu^{2+} ions might be used in low amounts (doping) compatible with some polyphenols, but careful analysis will be necessary. Furthermore, ions of copper and iron can catalyze Fenton-like reactions inducing oxidative stress in cells [11,65], being thus counterproductive to typical polyphenol bioactivity, although these metal-alginates may be useful looking for cytotoxic/anticancer actions [6,65].

As for calcium, barium and zinc ions, we excluded the hypothesis that they react substantially with common polyphenols and decided to proceed the development of metal-alginate delivery systems using these crosslinking ions.

3.4. Metal alginate matrices for controlled release of flavonoids

A convenient alginate-based delivery system was conceived consisting on dry alginate films that can be gelled and loaded with the bioactive drug close to time of application. Dry films are easier to transport and maintain at simple point-of-care conditions, and this possibility to develop controllable polyphenol delivery systems could foster the therapeutic applications of these compounds and alginate-based materials. In this work, we investigated the delivery properties of alginate matrices crosslinked with Ca^{2+}, Ba^{2+} and Zn^{2+} ions, and epicatechin was selected for these studies as it is a prototypical flavonoid with important biological activities (as previously presented on Introduction section).

Dry alginate films were produced by casting technique and drying to obtain thin and thick films of 85 ± 12 and 202 ± 55 μm thicknesses, respectively. For the release studies, films with identical surface area were used, being epicatechin encapsulated in simultaneous to the gelation of the films with the different metal ions. Gelation was carried at 4 °C to favor the stability of the flavonoid (section 4.3) and the flavonoid release was followed in saline medium at room temperature. Fig. 7 shows representative kinetic profiles obtained. Details for the production of the alginate films, the release assays and the kinetic models tested are described in Methods section 2.5.

Independently of the gelling metal ion used, the thin films released epicatechin faster than the thick films (Fig. 7). Noticeably, the calcium-gelled matrices attained a higher cumulative release than zinc and barium alginates. In general, most of the flavonoid was released in the first hour, although the thick barium matrices significantly prolonged the kinetics of release (Fig. 7C). A previous study with alginate microparticles also indicated that crosslinking with $ZnCl_2$ delayed diffusional drug release compared to $CaCl_2$-alginate matrices [53]. It should be noted that the release assays of epicatechin-loaded films were always run along with a blank film prepared in the same way, but without the flavonoid, to control eventual interferences with epicatechin analysis (inset in Fig. 7C). Overall, the results demonstrated that the delivery systems here conceived are able to afford micromolar concentrations of flavonoids, as required for accepted pharmacological activity [4,6,11,15].

The release results were fitted to three kinetic models: first order, Korsmeyer-Peppas and Weibull models (equations (4)–(6) in section 2.5). According to the correlation coefficients, the Weibull model is the best to describe the experimental data (full kinetic curves), with the lower R^2_{adj} observed 0.877 (Table 2). Nevertheless, when we restricted the modeling analysis to the first hour release data, thus capturing the initial kinetics during which most of the flavonoid is released, and reducing the contribution of the plateau phase to the analysis, we found that the Korsmeyer-Peppas model also fitted rather well the release data (Table S.2). The first order model fitted satisfactorily some of the release curves, as exemplified in the inset in Fig. 7B, but was more limited (Table 2 and S.2).

The values of the Weibull parameter b inferior to 0.75 obtained for most films (Table 2 and S.2) indicate that the release mechanism is by Fickian diffusion [59]. The thick barium films seem an exception, with $0.75 < b < 1$ pointing to a combined mechanism of Fickian diffusion and case II transport. The low values of n in the Korsmeyer-Peppas model (< 0.5) also suggest a simple diffusion mechanism for most films, whereas the $n > 0.5$ reinforce a more complex mechanism occurring with thick barium films [66]. The barium thick films lack the release properties suitable for typical polyphenol dermal treatments of a few hours, like Veregen® treatments, but it is remarkable that the thick films exhibited kinetics that depended strongly on the crosslinking metal, opening a possibility to tune alginate delivery systems for other applications.

3.5. Delivery of epicatechin on skin by easy-to-use alginate patch

The system devised in the previous section was assessed on a skin *ex vivo* model. Since calcium alginate films afforded the higher flavonoid concentrations in the preceding release assays (Fig. 7), calcium was chosen to crosslink the alginate films tested in skin. Alginate films were loaded with epicatechin and applied on porcine skin (Fig. 8A). The patch was applied over the small incision in the skin so that released epicatechin could contact with injured dermis. As dermal fibroblasts are known to metabolize polyphenols and some metabolites retain capacity to protect against oxidant skin-damaging conditions [20,67], we aimed to evaluate the presence of unmodified and antioxidant functional epicatechin after the topical application.

Samples were collected from skin surface 1 h after the application of alginate films and HPLC analysis confirmed the presence of significant levels of epicatechin deposited on the skin (Fig. 8 and Figure S.4). Tests were run in parallel with blank films (no epicatechin loaded) and, in these samples, no chromatographic peaks confoundable with epicatechin were detected (Figure S.4). These same samples collected from skin treated with blank films showed no measurable antioxidant activity by the cytochrome *c* reduction assay, while the epicatechin-loaded films afforded a significant antioxidant activity, as indicated by the rate of cytochrome *c* reduction induced by the sample (Fig. 8B).

Panel C in Fig. 8 summarizes the quantification of the flavonoid (50.0 ± 17.2 μM) and antioxidant bioactivity measured in the samples from skin treated with epicatechin-loaded films. The antioxidant activity of these samples seems tightly related to their epicatechin level, as the reduction rates are almost identical for blank samples spiked with the flavonoid (as described in methods) prior to cytochrome *c* assay (Fig. 8B). It should be noted that reduction of cytochrome *c* is a potential mechanism of action of flavonoids in cells [12], so the present results demonstrate that the alginate patch is able to deliver significant amounts of functionally active epicatechin on skin.

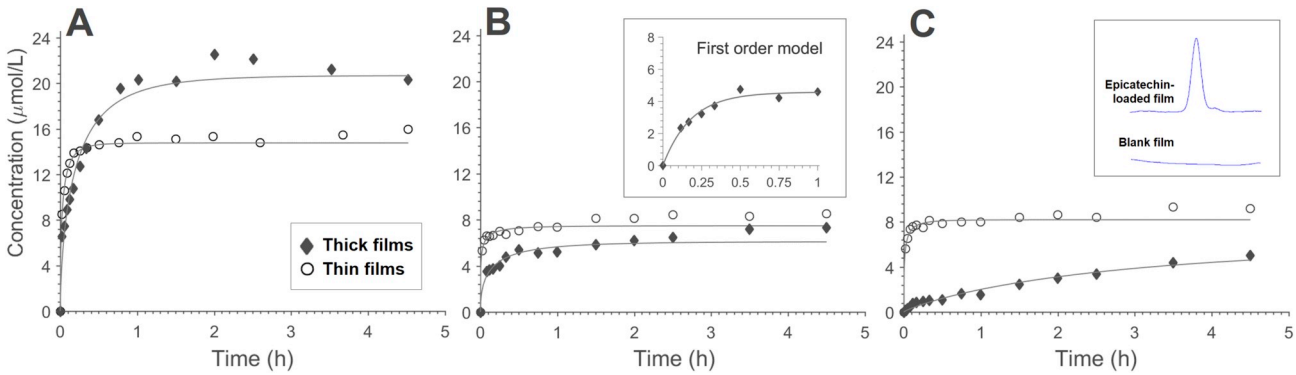

Fig. 7. Profiles of epicatechin release by calcium (A), zinc (B) and barium (C) alginate films in saline medium. The kinetic profiles shown are representative of triplicate encapsulation and release assays. Lines in the main plots are the best nonlinear regression fits of the experimental data to the Weibull kinetic model. Inset in panel B shows the fit of an initial release profile (first hour, thick zinc film) to the first order kinetic model. Insets in panel C show HPLC chromatographic peak (retention time 14 min) illustrating the analysis of epicatechin in the release media from loaded and unloaded blank films (thick barium films).

Table 2
Kinetic model parameters for epicatechin release by different metal alginate films. First order, Korsmeyer-Peppas and Weibull models were tested by non-linear regression and R^2_{adj} is the lowest (adjusted) coefficient of determination obtained from the curves for each film type.

Condition		First order		Korsmeyer-Peppas			Weibull		
		k (h^{-1})	R^2_{adj}	k (h^{-n})	n	R^2_{adj}	a (h^{-b})	b	R^2_{adj}
Ca^{2+}	Thick	6.80	0.826	0.89	0.21	0.898	2.87	0.79	0.934
	Thin	25.60	0.963	0.99	0.11	0.764	10.21	0.68	0.988
Zn^{2+}	Thick	3.83	0.819	0.85	0.21	0.869	2.66	0.69	0.877
	Thin	22.52	0.879	0.95	0.13	0.871	6.10	0.57	0.908
Ba^{2+}	Thick	0.33	0.949	0.28	0.69	0.947	0.34	0.94	0.946
	Thin	40.76	0.882	1.01	0.07	0.918	6.76	0.46	0.886

Epicatechin shares drug descriptors such as molecular weight (290 g/mol), hydrophobicity (logP > 0.5) or redox potential (E = 0.33 V) similar to many flavonoids, hence the delivery system here proposed is probably useful for the topical application of flavonoids in general. The epicatechin levels reached on skin surface suggest the future testing of this system in anticancer (melanoma) therapies for which simulation models predict that skin surface concentrations below 100 μM can be effective [6,19].

4. Conclusions

The studies carried in this work give additional support to the production of more diverse polyphenol-containing alginate biomaterials and development of alginate-based flavonoid delivery systems. Viscosity studies with alginate from two different suppliers indicate that modulation of the ionic composition (e.g. NaCl) is a simple and effective way to adjust viscosity properties of alginate solutions, which may prove useful to control the spinnability and printability of the biopolymer. Gelation studies with diverse metal cations showed that calcium, barium and zinc are the most suitable to produce morphologically regular and mechanically resistant gels. Syneresis upon gelation (water expulsion and mass reduction) increased in the order: $Fe^{2+} \approx Fe^{3+} < Cu^{2+} < Ca^{2+} \approx Ba^{2+} < Zn^{2+}$, independently of starting with alginate solutions 1% or 2% (w/v). The distinct results observed with both iron and copper-induced gelation are not a consequence of the pH of the crosslinking solutions of these acid metal ions.

Copper and iron ions should be avoided in the production of polyphenol-loaded materials because they react with the load, but calcium, barium and zinc can be used in alginates encapsulating typical compounds such as gallic acid, epicatechin and EGCG. Epicatechin loaded into alginate films crosslinked with Ca^{2+}, Ba^{2+} or Zn^{2+} is released by a kinetics dependent on the crosslinking ion and the film thicknesses. Diffusional release is the predominant mechanism and kinetics can be modeled using the Weibull equation. The easy-to-use alginate patch

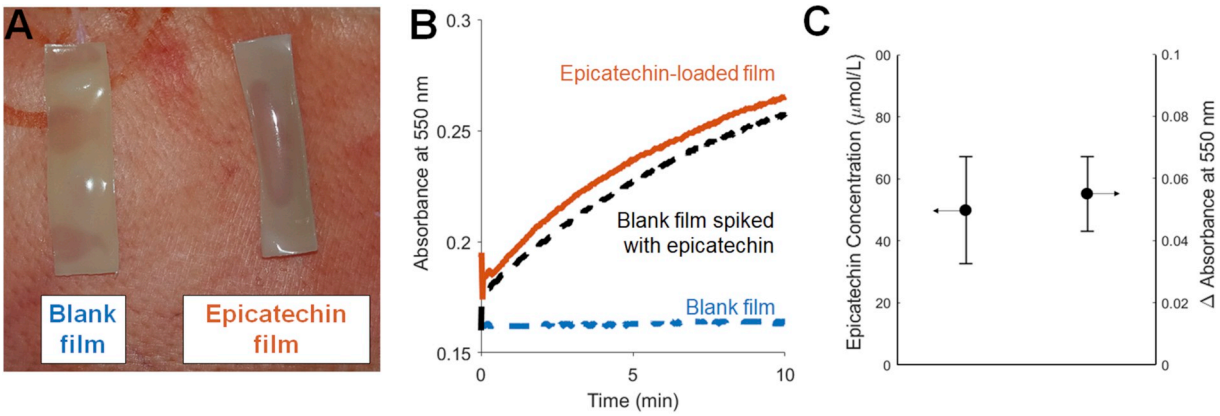

Fig. 8. Topical delivery of antioxidant epicatechin on porcine skin *ex vivo*. Epicatechin-loaded calcium alginate film applied on skin (A), and cytochrome *c* reducing activity of skin surface sampled 1 h after film application in comparison to skin treated with unloaded (blank) film (B). A kinetic curve of cytochrome *c* reduction by a blank sample spiked with epicatechin is also displayed. Panel C presents the quantification of epicatechin levels measured by HPLC and the cytochrome *c* reductive activity (absorbance increase after 10 min assay) of the samples from skin surface after 1-h application of epicatechin-loaded films. The results shown are representative experimental traces or the mean ± SE from delivery assays using skin from three different animals (n = 3).

here proposed was able to readily deliver therapeutically relevant concentrations of antioxidant functional epicatechin on skin, offering a novel and practical option for flavonoid-based therapies.

CRediT authorship contribution statement

João Silva: Investigation, Visualization, Writing - review & editing. **Pavlo Vanat:** Investigation. **Dorinda Marques-da-Silva:** Methodology, Investigation, Writing - review & editing. **Joaquim Rui Rodrigues:** Conceptualization, Writing - review & editing. **Ricardo Lagoa:** Conceptualization, Visualization, Writing - original draft, Writing - review & editing.

Declaration of competing interest

The authors declare no conflict of interest.

Acknowledgments

Authors acknowledge the support by “Fundação para a Ciência e Tecnologia” (FCT – Portugal) through the research project PTDC/BIA-MIB/31864/2017.

Appendix A. Supplementary data

Supplementary data to this article can be found online at https://doi.org/10.1016/j.bioactmat.2020.03.012.

References

[1] A. Shavandi, A.E.D.A. Bekhit, P. Saeedi, Z. Izadifar, A.A. Bekhit, A. Khademhosseini, Polyphenol uses in biomaterials engineering, Biomaterials 197 (2018) 91–106, https://doi.org/10.1016/j.biomaterials.2018.03.018.

[2] A. Sayed Abdelgeliel, S. Ferraris, A. Cochis, S. Vitalini, M. Iriti, H. Mohammed, A. Kumar, M. Cazzola, W.M. Salem, E. Verné, S. Spriano, L. Rimondini, Surface functionalization of bioactive glasses with polyphenols from padina pavonica algae and in situ reduction of silver ions: physico-chemical characterization and biological response, Coatings 9 (2019) 394, https://doi.org/10.3390/coatings9060394.

[3] X. Du, L. Wu, H. Yan, L. Qu, L. Wang, X. Wang, S. Ren, D. Kong, L. Wang, Multifunctional hydrogel patch with toughness, tissue adhesiveness, and antibacterial activity for sutureless wound closure, ACS Biomater. Sci. Eng. 5 (2019) 2610–2620, https://doi.org/10.1021/acsbiomaterials.9b00130.

[4] L. Shan, G. Gao, W. Wang, W. Tang, Z. Wang, Z. Yang, W. Fan, G. Zhu, K. Zhai, O. Jacobson, Y. Dai, X. Chen, Self-assembled green tea polyphenol-based coordination nanomaterials to improve chemotherapy efficacy by inhibition of carbonyl reductase 1, Biomaterials 210 (2019) 62–69, https://doi.org/10.1016/j.biomaterials.2019.04.032.

[5] J. Wang, W. Sang, Z. Yang, Z. Shen, Z. Wang, O. Jacobson, Y. Chen, Y. Wang, M. Shao, G. Niu, Y. Dai, X. Chen, Polyphenol-based nanoplatform for MRI/PET dual-modality imaging guided effective combination chemotherapy, J. Mater. Chem. B. 7 (2019) 5688–5694, https://doi.org/10.1039/c9tb01597c.

[6] R. Lagoa, J. Silva, J. Rodrigues, A. Bishayee, Advances in phytochemical delivery systems for improved anticancer activity, Biotechnol. Adv. 38 (2020) 107382, , https://doi.org/10.1016/j.biotechadv.2019.04.004.

[7] H. Yu, Z. Guo, S. Wang, G.S.N. Fernando, S. Channa, A. Kazlauciunas, D.P. Martin, S.A. Krasnikov, A. Kulak, C. Boesch, N.N. Sergeeva, Fabrication of hybrid materials from titanium dioxide and natural phenols for efficient radical scavenging against oxidative stress, ACS Biomater. Sci. Eng. 5 (2019) 2778–2785, https://doi.org/10.1021/acsbiomaterials.9b00535.

[8] M. Türk, S. Karahan, M. Çinar, Ş. Küçük, G.Ç. Dinçel, Characterization of chondrocytes cultured on catechin-loaded alginate-chitosan scaffolds, Artif. Cells, Nanomedicine Biotechnol. 41 (2013) 240–248, https://doi.org/10.3109/10731199.2012.718283.

[9] P. Wang, F. Zhang, Q. He, J. Wang, H.T. Shiu, Y. Shu, W.P. Tsang, S. Liang, K. Zhao, C. Wan, Flavonoid compound icariin activates hypoxia inducible factor-1α in chondrocytes and promotes articular cartilage repair, PloS One 11 (2016) e0148372, , https://doi.org/10.1371/journal.pone.0148372.

[10] X. Cheng, K. Li, S. Xu, P. Li, Y. Yan, G. Wang, Z. Berman, R. Guo, J. Liang, S. Traore, X. Yang, Applying chlorogenic acid in an alginate scaffold of chondrocytes can improve the repair of damaged articular cartilage, PloS One 13 (2018) e0195326, , https://doi.org/10.1371/journal.pone.0195326.

[11] D. Aluani, V. Tzankova, M. Kondeva-Burdina, Y. Yordanov, E. Nikolova, F. Odzhakov, A. Apostolov, T. Markova, K. Yoncheva, Evaluation of biocompatibility and antioxidant efficiency of chitosan-alginate nanoparticles loaded with quercetin, Int. J. Biol. Macromol. 103 (2017) 771–782, https://doi.org/10.1016/j.ijbiomac.2017.05.062.

[12] R. Lagoa, A.K. Samhan-Arias, C. Gutierrez-Merino, Correlation between the potency of flavonoids for cytochrome c reduction and inhibition of cardiolipin-induced peroxidase activity, Biofactors 43 (2017) 451–468, https://doi.org/10.1002/biof.1357.

[13] C. Gutierrez-Merino, C. Lopez-Sanchez, R. Lagoa, A.K. Samhan-Arias, C. Bueno, V. Garcia-Martinez, Neuroprotective actions of flavonoids, Curr. Med. Chem. 18 (2011) 1195–1212, https://doi.org/10.2174/092986711795029735.

[14] B.H. Kroes, A.J.J. Van Den Berg, H.C. Quarles Van Ufford, H. Van Dijk, R.P. Labadie, Anti-inflammatory activity of gallic acid, Planta Med. 58 (1992) 499–504, https://doi.org/10.1055/s-2006-961535.

[15] M. Inoue, R. Suzuki, N. Sakaguchi, Z. Li, T. Takeda, Y. Ogihara, B.Y. Jiang, Y. Chen, Selective induction of cell death in cancer cells by gallic acid, Biol. Pharm. Bull. 18 (1995) 1526–1530, https://doi.org/10.1248/bpb.18.1526.

[16] N.P. Bondonno, J.R. Lewis, L.C. Blekkenhorst, C.P. Bondonno, J.H. Shin, K.D. Croft, R.J. Woodman, G. Wong, W.H. Lim, B. Gopinath, V.M. Flood, J. Russell, P. Mitchell, J.M. Hodgson, Association of flavonoids and flavonoid-rich foods with all-cause mortality: the Blue Mountains Eye Study, Clin. Nutr. 39 (2019) 141–150, https://doi.org/10.1016/j.clnu.2019.01.004.

[17] J.M. Jeter, T.L. Bowles, C. Curiel-Lewandrowski, S.M. Swetter, F.V. Filipp, Z.A. Abdel-Malek, L.J. Geskin, J.D. Brewer, J.L. Arbiser, J.E. Gershenwald, E.Y. Chu, J.M. Kirkwood, N.F. Box, P. Funchain, D.E. Fisher, K.L. Kendra, A.A. Marghoob, S.C. Chen, M.E. Ming, M.R. Albertini, J.T. Vetto, K.A. Margolin, S.L. Pagoto, J.L. Hay, D. Grossman, D.L. Ellis, M. Kashani-Sabet, A.R. Mangold, S.N. Markovic, K.C. Nelson, J.G. Powers, J.K. Robinson, D. Sahni, A. Sekulic, V.K. Sondak, M.L. Wei, J.S. Zager, R.P. Dellavalle, J.A. Thompson, M.A. Weinstock, S.A. Leachman, P.B. Cassidy, Chemoprevention agents for melanoma: a path forward into phase 3 clinical trials, Cancer 125 (2019) 18–44, https://doi.org/10.1002/cncr.31719.

[18] J. Kessels, L. Voeten, P. Nelemans, J. Cleutjens, L.M. Hillen, K. Mosterd, N.W.J. Kelleners-Smeets, Topical sinecatechins, 10%, ointment for superficial basal cell carcinoma: a randomized clinical trial, JAMA Dermatology 153 (2017) 1061–1063, https://doi.org/10.1001/jamadermatol.2017.2529.

[19] J. Silva, P. Videira, R. Lagoa, Bioactivity gradients of cytoprotective and anticancer catechins in skin: simulation studies for the design of controlled release systems, ENBENG 2017 - 5th Port. Meet. Bioeng. Proc, 2017, https://doi.org/10.1109/ENBENG.2017.7889467.

[20] S. Basu-Modak, M.J. Gordon, L.H. Dobson, J.P.E. Spencer, C. Rice-Evans, R.M. Tyrrell, Epicatechin and its methylated metabolite attenuate UVA-induced oxidative damage to human skin fibroblasts, Free Radic. Biol. Med. 35 (2003) 910–921, https://doi.org/10.1016/S0891-5849(03)00436-2.

[21] K.A. Clarke, T.P. Dew, R.E.B. Watson, M.D. Farrar, J.E. Osman, A. Nicolaou, L.E. Rhodes, G. Williamson, Green tea catechins and their metabolites in human skin before and after exposure to ultraviolet radiation, J. Nutr. Biochem. 27 (2016) 203–210, https://doi.org/10.1016/j.jnutbio.2015.09.001.

[22] I. Megow, M.E. Darvin, M.C. Meinke, J. Lademann, A randomized controlled trial of green tea beverages on the in vivo radical scavenging activity in human skin, skin pharmacol, Physiol. 30 (2017) 225–233, https://doi.org/10.1159/000477355.

[23] J.I. Dower, J.M. Geleijnse, L. Gijsbers, C. Schalkwijk, D. Kromhout, P.C. Hollman, Supplementation of the pure flavonoids epicatechin and quercetin affects some biomarkers of endothelial dysfunction and inflammation in (Pre)Hypertensive adults: a randomized double-blind, placebo-controlled, crossover trial, J. Nutr. 145 (2015) 1459–1463, https://doi.org/10.3945/jn.115.211888.

[24] R. Bahramsoltani, F. Ebrahimi, M.H. Farzaei, A. Baratpourmoghaddam, P. Ahmadi, P. Rostamiasrabadi, A.H. Rasouli Amirabadi, R. Rahimi, Dietary polyphenols for atherosclerosis: a comprehensive review and future perspectives, Crit. Rev. Food Sci. Nutr. 59 (2019) 114–132, https://doi.org/10.1080/10408398.2017.1360244.

[25] D. Milenkovic, K. Declerck, Y. Guttman, Z. Kerem, S. Claude, A.R. Weseler, A. Bast, H. Schroeter, C. Morand, W. Vanden Berghe, (−)-Epicatechin metabolites promote vascular health through epigenetic reprogramming of endothelial-immune cell signaling and reversing systemic low-grade inflammation, Biochem. Pharmacol. 173 (2020) 113699, , https://doi.org/10.1016/j.bcp.2019.113699.

[26] A.M. Emara, H. El-Bahrawy, Green tea attenuates benzene-induced oxidative stress in pump workers, J. Immunot. 5 (2008) 69–80, https://doi.org/10.1080/15476910802019029.

[27] H.A. Oketch-Rabah, A.L. Roe, C.V. Rider, H.L. Bonkovsky, G.I. Giancaspro, V. Navarro, M.F. Paine, J.M. Betz, R.J. Marles, S. Casper, B. Gurley, S.A. Jordan, K. He, M.P. Kapoor, T.P. Rao, A.H. Sherker, R.J. Fontana, S. Rossi, R. Vuppalanchi, L.B. Seeff, A. Stolz, J. Ahmad, C. Koh, J. Serrano, T. Low Dog, R. Ko, United States Pharmacopeia (USP) comprehensive review of the hepatotoxicity of green tea extracts, Toxicol. Reports. 7 (2020) 386–402, https://doi.org/10.1016/j.toxrep.2020.02.008.

[28] K.Y. Lee, D.J. Mooney, Alginate: properties and biomedical applications, Prog. Polym. Sci. 37 (2012) 106–126, https://doi.org/10.1016/j.progpolymsci.2011.06.003.

[29] S. Stratton, N.B. Shelke, K. Hoshino, S. Rudraiah, S.G. Kumbar, Bioactive polymeric scaffolds for tissue engineering, Bioact. Mater. 1 (2016) 93–108, https://doi.org/10.1016/j.bioactmat.2016.11.001.

[30] M.P. Nikolova, M.S. Chavali, Recent advances in biomaterials for 3D scaffolds: a review, Bioact. Mater. 4 (2019) 271–292, https://doi.org/10.1016/j.bioactmat.2019.10.005.

[31] M. Zare-Gachi, H. Daemi, J. Mohammadi, P. Baei, F. Bazgir, S. Hosseini-Salekdeh, H. Baharvand, Improving anti-hemolytic, antibacterial and wound healing properties of alginate fibrous wound dressings by exchanging counter-cation for infected full-thickness skin wounds, Mater. Sci. Eng. C 107 (2020) 110321, , https://doi.org/10.1016/j.msec.2019.110321.

[32] H.L. Jiang, Y.L. Cui, Y. Qi, Microencapsulation of rutin in chitosan-coated alginate

microspheres through internal gelation technique, Adv. Mater. Res. 716 (2013) 455–458 https://doi.org/10.4028/www.scientific.net/AMR.716.455.
[33] Y. Li, Y. Liu, C. Jiang, S. Li, G. Liang, Q. Hu, A reactor-like spinneret used in 3D printing alginate hollow fiber: a numerical study of morphological evolution, Soft Matter 12 (2016) 2392–2399, https://doi.org/10.1039/c5sm02733k.
[34] D. Yu, Z. Dong, H.T. Lim, Y. Chen, Z. Ding, N. Sultana, J. Wu, B. Qin, J. Cheng, W. Li, Microfluidic preparation, shrinkage, and surface modification of monodispersed alginate microbeads for 3D cell culture, RSC Adv. 9 (2019) 11101–11110, https://doi.org/10.1039/C9RA01443H.
[35] J. Rodrigues, R. Lagoa, Copper ions binding in Cu-alginate gelation, J. Carbohydr. Chem. 25 (2006) 219–232, https://doi.org/10.1080/07328300600732956.
[36] M.C. Straccia, G.G. D'Ayala, I. Romano, P. Laurienzo, Novel zinc alginate hydrogels prepared by internal setting method with intrinsic antibacterial activity, Carbohydr. Polym. 125 (2015) 103–112, https://doi.org/10.1016/j.carbpol.2015.03.010.
[37] S.H. Lim, H. Kathuria, J.J.Y. Tan, L. Kang, 3D printed drug delivery and testing systems — a passing fad or the future? Adv. Drug Deliv. Rev. 132 (2018) 139–168, https://doi.org/10.1016/j.addr.2018.05.006.
[38] S.N. Economidou, D.A. Lamprou, D. Douroumis, 3D printing applications for transdermal drug delivery, Int. J. Pharm. 544 (2018) 415–424, https://doi.org/10.1016/j.ijpharm.2018.01.031.
[39] Y. He, F. Yang, H. Zhao, Q. Gao, B. Xia, J. Fu, Research on the printability of hydrogels in 3D bioprinting, Sci. Rep. 6 (2016) 29977, , https://doi.org/10.1038/srep29977.
[40] A. Dodero, S. Vicini, M. Alloisio, M. Castellano, Sodium alginate solutions: correlation between rheological properties and spinnability, J. Mater. Sci. 54 (2019) 8034–8046, https://doi.org/10.1007/s10853-019-03446-3.
[41] J. Yang, S. Chen, Y. Fang, Viscosity study of interactions between sodium alginate and CTAB in dilute solutions at different pH values, Carbohydr. Polym. 75 (2009) 333–337, https://doi.org/10.1016/j.carbpol.2008.07.037.
[42] D. Zhong, X. Huang, H. Yang, R. Cheng, New insights into viscosity abnormality of sodium alginate aqueous solution, Carbohydr. Polym. 81 (2010) 948–952, https://doi.org/10.1016/j.carbpol.2010.04.012.
[43] Q. Xiao, Q. Tong, L.T. Lim, Pullulan-sodium alginate based edible films: rheological properties of film forming solutions, Carbohydr. Polym. 87 (2012) 1689–1695, https://doi.org/10.1016/j.carbpol.2011.09.077.
[44] A. Martinsen, G. Skjåk-Bræk, O. Smidsrød, F. Zanetti, S. Paoletti, Comparison of different methods for determination of molecular weight and molecular weight distribution of alginates, Carbohydr. Polym. 15 (1991) 171–193, https://doi.org/10.1016/0144-8617(91)90031-7.
[45] M.R. Torres, A.P.A. Sousa, E.A.T. Silva Filho, D.F. Melo, J.P.A. Feitosa, R.C.M. de Paula, M.G.S. Lima, Extraction and physicochemical characterization of Sargassum vulgare alginate from Brazil, Carbohydr. Res. 342 (2007) 2067–2074, https://doi.org/10.1016/j.carres.2007.05.022.
[46] L. Iskandar, L. Rojo, L. Di Silvio, S. Deb, The effect of chelation of sodium alginate with osteogenic ions, calcium, zinc, and strontium, J. Biomater. Appl. 34 (2019) 573–584, https://doi.org/10.1177/0885328219861904.
[47] E.S. Place, L. Rojo, E. Gentleman, J.P. Sardinha, M.M. Stevens, Strontium-and zinc-alginate hydrogels for bone tissue engineering, Tissue Eng. 17 (2011) 2713–2722, https://doi.org/10.1089/ten.tea.2011.0059.
[48] W. Klinkajon, P. Supaphol, Novel copper (II) alginate hydrogels and their potential for use as anti-bacterial wound dressings, Biomed. Mater. 9 (2014) 045008, , https://doi.org/10.1088/1748-6041/9/4/045008.
[49] I. Malagurski, S. Levic, M. Mitric, V. Pavlovic, S. Dimitrijevic-Brankovic, Bimetallic alginate nanocomposites: new antimicrobial biomaterials for biomedical application, Mater. Lett. 212 (2018) 32–36, https://doi.org/10.1016/j.matlet.2017.10.046.
[50] L. Baldino, S. Cardea, M. Scognamiglio, E. Reverchon, A new tool to produce alginate-based aerogels for medical applications, by supercritical gel drying, J. Supercrit. Fluids 146 (2019) 152–158, https://doi.org/10.1016/j.supflu.2019.01.016.
[51] D.C. Bassett, I. Madzovska, K.S. Beckwith, T.B. Melø, B. Obradovic, P. Sikorski, Dissolution of copper mineral phases in biological fluids and the controlled release of copper ions from mineralized alginatehydrogels, Biomed. Mater. 10 (2015) 015006, , https://doi.org/10.1088/1748-6041/10/1/015006.
[52] V. Pillay, M.P. Danckwerts, Z. Muhidinov, R. Fassihi, Novel modulation of drug delivery using binary zinc-alginate-pectinate polyspheres for zero-order kinetics over several days: experimental design strategy to elucidate the crosslinking mechanism, Drug Dev. Ind. Pharm. 31 (2005) 191–207, https://doi.org/10.1081/DDC-200047806.
[53] S.M. Jay, W.M. Saltzman, Controlled delivery of VEGF via modulation of alginate microparticle ionic crosslinking, J. Contr. Release 134 (2009) 26–34, https://doi.org/10.1016/j.jconrel.2008.10.019.
[54] B.L. Strand, Y.A. Mørch, K.R. Syvertsen, T. Espevik, G. Skjåk-Bræk, Microcapsules made by enzymatically tailored alginate, J. Biomed. Mater. Res. 64 (2003) 540–550.
[55] B. Sarmento, A.J. Ribeiro, F. Veiga, D.C. Ferreira, R.J. Neufeld, Insulin-loaded nanoparticles are prepared by alginate lonotropic pre-gelation followed by chitosan polyelectrolyte complexation, J. Nanosci. Nanotechnol. 7 (2007) 2833–2841, https://doi.org/10.1166/jnn.2007.609.
[56] H. Zhang, H. Wang, J. Wang, R. Guo, Q. Zhang, The effect of ionic strength on the viscosity of sodium alginate solution, Polym. Adv. Technol. 12 (2001) 740–745, https://doi.org/10.1002/pat.97.
[57] W.S. Rasband, ImageJ, US National Institutes of Health, Bethesda, MD, 1997Http://Rsb.Info.Nih.Gov/Ij.
[58] P. Ganesan, C.S. Kumar, N. Bhaskar, Antioxidant properties of methanol extract and its solvent fractions obtained from selected Indian red seaweeds, Bioresour, Technol. 99 (2008) 2717–2723, https://doi.org/10.1016/j.biortech.2007.07.005.
[59] V. Papadopoulou, K. Kosmidis, M. Vlachou, P. Macheras, On the use of the Weibull function for the discernment of drug release mechanisms, Int. J. Pharm. 309 (2006) 44–50, https://doi.org/10.1016/j.ijpharm.2005.10.044.
[60] H.F. Chan, R. Zhao, G.A. Parada, H. Meng, K.W. Leong, L.G. Griffith, X. Zhao, Folding artificial mucosa with cell-laden hydrogels guided by mechanics models, Proc. Natl. Acad. Sci. U.S.A. 115 (2018) 7503–7508, https://doi.org/10.1073/pnas.1802361115.
[61] M. Matyash, F. Despang, C. Ikonomidou, M. Gelinsky, Swelling and mechanical properties of alginate hydrogels with respect to promotion of neural growth, Tissue Eng. C Methods 20 (2014) 401–411, https://doi.org/10.1089/ten.tec.2013.0252.
[62] H. Andriamanantoanina, M. Rinaudo, Relationship between the molecular structure of alginates and their gelation in acidic conditions, Polym. Int. 59 (2010) 1531–1541, https://doi.org/10.1002/pi.2943.
[63] Y. Qi, M. Jiang, Y.L. Cui, L. Zhao, X. Zhou, Synthesis of quercetin loaded nanoparticles based on alginate for Pb(II) adsorption in aqueous solution, Nanoscale Res. Lett. 10 (2015) 408, https://doi.org/10.1186/s11671-015-1117-7.
[64] Y. Wei, M. Guo, Zinc-Binding sites on selected flavonoids, Biol. Trace Elem. Res. 161 (2014) 223–230, https://doi.org/10.1007/s12011-014-0099-0.
[65] K. Du, Q. Liu, M. Liu, R. Lv, N. He, Z. Wang, Encapsulation of glucose oxidase in Fe (III)/tannic acid nanocomposites for effective tumor ablation via Fenton reaction, Nanotechnology (2020), https://doi.org/10.1088/1361-6528/ab44f9.
[66] J. Siepmann, N.A. Peppas, Modeling of drug release from delivery systems based on hydroxypropyl methylcellulose (HPMC), Adv. Drug Deliv. Rev. 64 (2012) 163–174, https://doi.org/10.1016/j.addr.2012.09.028.
[67] J.P.E. Spencer, G.G.C. Kuhnle, R.J. Williams, C. Rice-Evans, Intracellular metabolism and bioactivity of quercetin and its in vivo metabolites, Biochem. J. 372 (2003) 173–181, https://doi.org/10.1042/BJ20021972.